Journal of Hydrology 529 (2015) 1562–1577

Contents lists available at ScienceDirect

Journal of Hydrology

journal homepage: www.elsevier.com/locate/jhydrol

Hydrology, sediment circulation and long-term morphological changes in highly urbanized Shenzhen River estuary, China: A combined field experimental and modeling approach

Shiyan Zhang [a,b], Xian-zhong Mao [a,*]

[a] Division of Ocean Science and Technology, Graduate School at Shenzhen, Tsinghua University, Shenzhen 518055, China
[b] Key Laboratory of Water Cycle and Related Land Surface Processes, Institute of Geographic Sciences and Natural Resources Research, Chinese Academy of Sciences, Beijing 100101, China

ARTICLE INFO

Article history:
Received 1 September 2014
Received in revised form 18 March 2015
Accepted 14 August 2015
Available online 20 August 2015
This manuscript was handled by Laurent Charlet, Editor-in-Chief, with the assistance of Nicolas Gratiot, Associate Editor

Keywords:
Sediment circulation
Morphological process
Hydrographic survey
Long-term simulation
DELFT model
Rapid urbanization

SUMMARY

The Shenzhen River estuary is a small estuary in highly urbanized regions between Shenzhen and Hong Kong, China. An increasing amount of sediment has been observed to accumulate in the estuary, imposing a severe impact on the ecological environment. In this study we utilized a series of hydrographic and bathymetry surveys to study the hydrology, sediment transport and morphological processes in the estuary. Flow and sediment circulation patterns in different seasons were inferred using current velocity, salinity and suspended sediment concentration (SSC) time series collected in the hydrographic surveys in conjunction with fathometer profiles in bathymetry surveys. Historical time series at two stations were also analyzed by Mann–Kendall test for possible trends of the driving forces for estuarine morphological processes. The two-dimensional depth-averaged DELFT numerical model was employed to simulate the flow, salinity and SSC fields during the synchronous surveys and to predict the long-term morphological processes in the estuary. A bimodal SSC distribution was observed with two high-SSC zones separated by a low-SSC zone near the central bay, which cannot be explained by the conventional nongravitational transport theory of Postma (1967). It is hypothesized that sediment circulation in the estuary can be separated into two different systems: the "tidal zone" is under the influence of marine sediment from the Pearl River estuary, whereas the "fluvial zone" is mainly affected by terrestrial sediment from the river. Sediment mass exchange between the two systems is limited due to the presence of the low-SSC zone, the location of which could vary with the relative strengths of river flow and tides. The trend analysis of historical time series shows that the river discharge and the mean sea level are increasing and the flood tide range and the ebb tide range are decreasing. These trends are closely related to the intense human activities in the urbanization of Shenzhen. The long-term simulations show depositional trends for the inner bay and the coastline of the outer bay, which could be further aggravated by the detected trends of the driving forces.

1. Introduction

Sediment deposition is one of the major environmental concerns for estuaries. Due to channel widening and saline intrusion, sediment particles are prone to settling in estuaries, and severe sediment deposition is frequently observed. Heavy sediment deposition may cause significant morphological changes, which in turn alter the ecological environment of the estuary. Furthermore, deposited sediment once contaminated by polluted water becomes a potential source of hazardous chemicals when surface water quality is restored. Sediment deposition in an estuary can be highly variable when the estuary is strongly disturbed by certain factors, such as land reclamation in the estuary or other human activities in its catchment.

The Shenzhen River estuary experienced severe sediment deposition in recent decades. The estuary lies on the boundary of Shenzhen and Hong Kong, and is connected with the South China Sea via the Pearl River estuary. Two important nature conservation sites are located at the river mouth in the estuary: Futian Mangrove-bird Nature Reserve, one of the few mangrove sites in China, is located on its north side and Mai Po Marshes Nature Reserve, a RAMSAR site declared in 1995, is located on its south

* Corresponding author.
E-mail addresses: zhangshy@igsnrr.ac.cn (S. Zhang), maoxz@sz.tsinghua.edu.cn (X.-z. Mao).

http://dx.doi.org/10.1016/j.jhydrol.2015.08.027
0022-1694/

side. Since the late 1970s, Shenzhen has experienced rapid growth in its population and economy. Permanent residents in Shenzhen increased from 0.37 million in 1981 to 10.55 million in 2012 and the Gross Domestic Product increased from 0.5 billion RMB in 1981 to 1295.0 billion RMB in 2012 (NBSC, 2012). At the same time, large volumes of sediment have been observed to rapidly accumulate in the estuary. Shenzhen and Hong Kong have launched a series of regulation projects to remediate sediment deposition in the estuary. Hydrographic surveys have been carried out regularly in order to explore the hydrology and sediment transport in the estuary since the 1990s. However, few studies have been reported in the literature for this region.

Sediment transport and related morphological processes in estuaries have long been investigated by scientists and coastal engineers (Carling, 1982; Harris and Collins, 1984; Fenster and FitzGerald, 1996; Woodruff et al., 2001; Uncles and Stephens, 2010, among others). Several surveying techniques, including hydrographic surveying, sonar scanning, field sampling and sediment coring, were widely used in estuarine field studies. For example, Carling (1982) measured current and wave dynamics, sediment properties, SSC and sedimentation rates at fixed stations to study their temporal and spatial variations, and discussed the links between sediment resuspension and sedimentation rates for an intertidal zone in South Wales. Fenster and FitzGerald (1996) used several types of survey data including fathometer profiles, side-scan sonograms, hydrographic data, seismic profiles and bridge borings to synthetically study the sediment circulation and its morphological responses in the lower Kennebec River estuary in the USA. The SSC distribution in an estuary is often characterized by the existence of a "turbidity maximum", where the SSC is significantly higher than that in the upstream and downstream regions. Although several theories have been proposed for the formation of turbidity maximum (Postma, 1967; Festa and Hansen, 1978; Simpson et al., 1990; Stacey et al., 2001; Lerczak and Geyer, 2004; Burchard and Hetland, 2010; Ralston et al., 2012; Geyer and MacCready, 2014), it remains a difficult task to clarify the estuarine sediment circulation pattern due to its complex nature. Intensive data have been collected from the hydrographic and bathymetry surveys performed in the Shenzhen River estuary, thereby offering an excellent opportunity for studying the hydrology, sediment transport and morphological processes.

When investigated on a larger time scale, field data might not be sufficient for small estuaries with short survey histories such as the Shenzhen River estuary. Under such circumstances, numerical models can be used as a supplementary tool in analyzing the long-term processes. Attempts to investigate the sediment transport and morphological processes with numerical models have been made in a variety of studies of different time scales (for example, see Cao et al., 2002; Wu, 2004; El kadi Abderrezzak and Paquier, 2009; Chen et al., 2010; Zhang and Duan, 2011; among others). These models, sometimes called "process-based" models because they solve coupled systems of hydrodynamic equations and sediment transport equations, successfully reproduced the fluvial processes in event-based simulations. However, quantitative predictions of morphological processes on larger time scales such as years or decades remain a challenging task for several reasons: (1) the computational time steps in process-based models are usually limited to a few minutes or even seconds due to stability consideration; (2) the error accumulation effect causes the model results to deviate from true solutions; (3) morphological changes are often in response to extreme events which are stochastic; and (4) morphological evolution may be chaotic in nature. Nonetheless, recent studies (Cayocca, 2001; Lesser et al., 2004; Seybold et al., 2009; Mariotti and Fagherazzi, 2010) using numerical models in long-term morphodynamic simulations showed promising results, encouraging the use of a numerical model in exploring the long-term morphological processes in the Shenzhen River estuary. The DELFT model developed by DELTARES (previously known as Delft Hydraulics, Lesser et al., 2004) has been proposed in many studies (Lesser et al., 2004; Dastgheib et al., 2008; Van der Wegen et al., 2011), and is used in the present study.

This paper presents the work carried out in recent hydrographic and bathymetry surveys in the Shenzhen River estuary. The objective of this study is to analyze the flow and sediment circulation pattern in the Shenzhen River estuary with recent survey data, and to predict the long-term trends of sediment deposition under different scenarios of driving force variations. The Shenzhen River estuary presents some unique sediment circulation patterns not possessed by other estuaries reported in the literature. Furthermore, intense human activities in the urbanization could seriously affect the river flow and tidal dynamics in the estuary, which may impose potential adverse impact on the estuarine morphological processes. The present study may help to understand the source and formation mechanism of sediment deposition in small urbanized estuaries with similar settings as the Shenzhen River estuary and to find possible solutions to control the estuarine sediment deposition.

2. Physical setting of the Shenzhen River estuary

The Shenzhen River estuary consists of the main stream of Shenzhen River and the entire Shenzhen Bay (Fig. 1). Shenzhen River is an urbanized tidal river connecting to the Pearl River estuary via Shenzhen Bay. The total length of Shenzhen River is 33 km, and the channel under tidal influence extends from the river mouth to about 13 km upstream. Major tributaries of Shenzhen River include Buji River, Futian River, Huanggang River, Xinzhou River, Wutong River, Shawan River and Liantang River (Dasha River and Yuen Long River flow directly into Shenzhen Bay). A summary of the tributaries are listed in Table 1. The catchment of Shenzhen River locates on the south of the heavily populated Pearl River Delta, covering a drainage area of 312.5 km^2, with 187.5 km^2 in Shenzhen (Chan and Lee, 2010). The northern (Shenzhen) side and the southern (Hong Kong) side of the catchment are distinctively different. On the north of the Shenzhen River it is primarily urbanized areas and on the south it is rural villages and wildland with relatively population density. The catchment has a warm and humid subtropical maritime monsoon climate, and the average annual rainfall between 1995 and 2009 is 1998.4 mm, producing an annual stream volume of 530×10^6 m^3, with over 85% occurring between April and September. Shenzhen Bay is located between latitudes 22.41°N and 22.53°N, longitudes 113.88° E and 114.00°E. It is 13.9 km long and between 4 and 8 km wide, covering an area of 85 km^2. The mean water depth is only 2.9 m in the inner bay and increases to over 7 m in the outer bay. The suspended sediment and the bottom sediment in the estuary are within the range of cohesive silt and clay, with coarser particles occasionally found near the bay mouth and river mouth. The Municipal Shenzhen River Regulation Office of Shenzhen measured the particle size distributions at a number of sites in the estuary (unpublished data), and found that the median sizes were 8–15 μm for suspended sediment and generally below 32 μm for bottom sediment. The tides in the estuary are semidiurnal with an average range of 1.4 m. Rapidly deposited sediment may gradually decrease the environmental capacity of the Shenzhen River estuary, which becomes a potential threat to the ecosystem in aquatic systems.

3. Data and methods

3.1. Data source

Survey data to be analyzed in the present study were summarized in Table 2. Three types of surveys were conducted by the

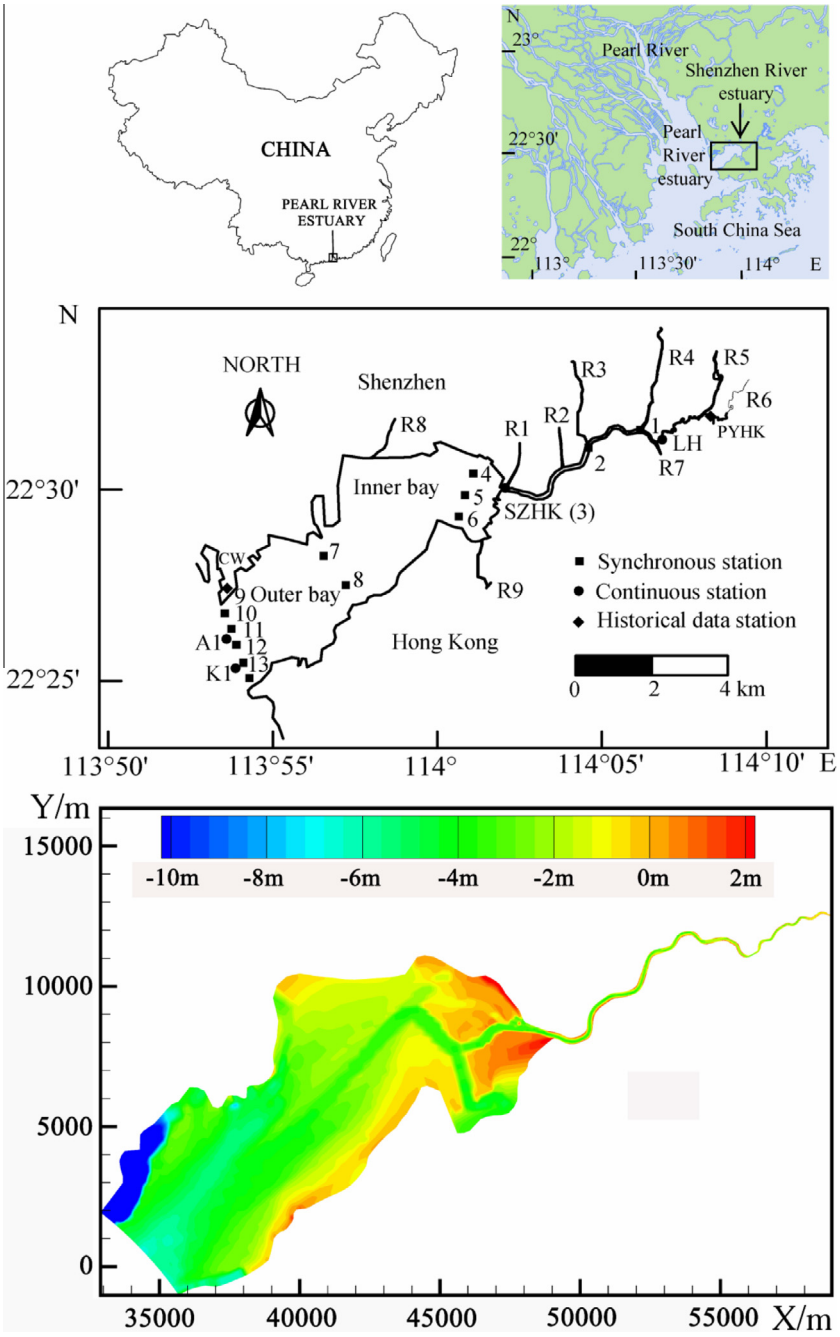

Fig. 1. Map of the Shenzhen River estuary (top), locations of survey stations (center) and bathymetry of the Shenzhen Bay (bottom). The coordinate system in the bathymetry chart is the local Shenzhen River estuary coordinate system (and sic passim). R1 = Xinzhou River; R2 = Huanggang River; R3 = Futian River; R4 = Buji River; R5 = Shawan River; R6 = Liantang River; R7 = Wutong River; R8 = Dasha River; R9 = Yuen Long River; 1–13 = Synchronous survey stations; LH, SZHK, CW, A1, K1 = continuous survey stations; PYHK, CW: historical data stations. Note that continuous survey station SZHK coincides with synchronous station 3. Continuous survey at the bay mouth is carried out at different locations, the water surface elevation is measured at CW and suspended sediment concentration (SSC) is measured at A1 and K1. SSC values used in the present study are averaged from data of A1 and K1.

Municipal Shenzhen River Regulation Office of Shenzhen, including the synchronous surveys, the continuous surveys and the bathymetry surveys. Additional historical time series were also used in detecting possible trends of the driving forces. Procedures for data collection are briefly described below.

3.1.1. Synchronous surveys

Four synchronous hydrographic surveys were carried out in October 17–18 of 2004 (representing spring tides with low river discharge), October 25–26 of 2004 (neap tides with low river discharge), June 16–17 of 2005 (neap tides with moderate river discharge) and June 23–24 of 2005 (spring tides with high river discharge). Current velocity, salinity and SSC were synchronously measured at a number of stations (13 in the dry season and 27 in the wet season). Data measured at six stations are presented in this study (see Fig. 1a): S1 and S2 are about 8.6 and 5.3 km upstream of the river mouth, S3 is at the river mouth, S5 is near the submarine channel in the inner bay, S7 is near the bay center and S11 is near the bay mouth. These stations are located approximately at the center of the cross sections and therefore able to represent the cross-sectional averages. At each station, the survey was performed for 28–29 h, with measurements taken every 30–

Table 1
Summary of tributaries of Shenzhen River and Shenzhen Bay. R1–R9 are the tributaries shown in Fig. 1. See the caption of Fig. 1 for the river names.

River	Length (km)	Drainage area (km^2)	Discharge (m^3/s)	Catchment land type
R1	7.82	19.8	0.278 (2009, upstream[a])	Urbanized
R2	1.72	3.0	No data	Urbanized
R3	9.93	15.40	0.761 (January to October 2005)	Urbanized
R4	21.0	63.47	4.60 (2009, upstream)	Urbanized
R5	20.84	68.70	>0.23[b] (1996)	Partly urbanized
R6	12.0	81.5	3.87 (2009)	Urbanized
R7	No data	No data	3.50 (2009)	Rural
R8	13.5	90.7	4.27 (2008)	Urbanized
R9	14.3	29.2	No data	Partly urbanized

[a] The contents in the brackets denote time for the measurement of the discharge, *upstream* indicates the measurement is not taken at the confluence.
[b] The measurements were only taken in flooding times.

60 min. Current velocity was measured by the shipborne current velocimeters. Salinity was converted from electric conductivity readings measured with shipborne conductivimeters. SSC was measured by taking water samples, and then filtering, drying and weighing in the laboratory. Multiple measurements were taken at different depths to calculate the depth-averaged quantities according to the following criterion:

$$\overline{U} = \begin{cases} \dfrac{U_{0H}+U_{0.2H}+U_{0.4H}+U_{0.6H}+U_{0.8H}+U_{1H}}{10}, & H > 5\,\mathrm{m} \\ \dfrac{U_{0.2H}+U_{0.4H}+U_{0.6H}}{3}, & 2\,\mathrm{m} < H \leqslant 5\,\mathrm{m} \\ \dfrac{U_{0.2H}+U_{0.8H}}{2}, & 1.5\,\mathrm{m} < H \leqslant 2\,\mathrm{m} \\ U_{0.6H}, & 0.8\,\mathrm{m} < H \leqslant 1.5\,\mathrm{m} \\ U_{0.5H}, & H \leqslant 0.8\,\mathrm{m} \end{cases} \quad (1)$$

where $\overline{U}$ = depth-averaged quantities; H = water depth, U_{0H}, $U_{0.2H}$, $U_{0.4H}$, $U_{0.6H}$, $U_{0.8H}$, U_{1H} = values measured at 0, 0.2, 0.4, 0.6, 0.8 and 1 times the water depth from the water surface. Other ancillary data included the magnitude and the direction of prevailing wind and surface water temperature, which were measured with hand-held anemometers and thermometers.

3.1.2. Continuous surveys

Continuous surveys were performed at one bay station, Chi Wan (CW, located at the bay mouth), and two river stations, Luo Hu (LH, located about 10 km from the river mouth) and Shen Zhen He Kou (SZHK, located at the river mouth). Tide elevation and SSC at CW, current velocity and SSC at LH and SZHK were measured during the surveys. Tide elevation was recorded hourly with a pressure-type automatic water-level recorder. Current velocity was measured every 10 min with fixed-station ADCPs. The turbidity sensors were deployed approximately 0.6–0.8 times the water depth below the water surface at CW, and 0.5 m below water surface at LH and SZHK due to technical restrictions. The measuring frequency is 10 min at LH and SZHK, and 30 min at CW. Since the ADCPs and the turbidity sensors at LH and SZHK were installed in 2006, data from 2007 to 2009 were analyzed in the present study.

3.1.3. Bathymetry surveys

Regular bathymetry surveys for the Shenzhen River estuary have been carried out since 2001. Early surveys prior to 2007 only covered a small part of the inner bay and the river from km 0.0 to 9.9 (numbers denotes the distance in kilometer upstream of the river mouth). Since 2007, the entire bay and the river from km 0.0 to 13.4 have been covered. The river was surveyed twice each year before and after the wet season, and the bay was surveyed only once after the wet season. Water depth was recorded with a shipborne fathometer with a vertical precision of 1 cm, and then converted to bed elevation. There are three sets of bathymetric data collected: scattered bathymetric data, cross-sectional bathymetric profiles and longitudinal bathymetric profiles. The scattered bathymetric data are measured in both the river and the bay, and the cross-sectional bathymetric profiles and the longitudinal bathymetric profiles were measured only in the river. In the scattered bathymetric surveys, the sampling spacing was 5–10 m between two neighboring points in the same survey line, 10–20 m between two survey lines in the river, and 40–50 m between two survey lines in the bay. In the cross-sectional bathymetric surveys, the bed elevation was measured in fixed cross sections 100 m apart, and the sampling spacing in each cross section is 5–10 m. In the longitudinal bathymetric surveys, the bed elevation was measured approximately along the centerline of the river. In the present study, only the first two data sets collected from January 2008 to December 2009 are used.

3.1.4. Historical data

Historical time series used in the present study were compiled from surveys performed at two hydrographic stations near the

Table 2
Summary of survey data used in this study. V = current velocity; S = salinity; C = suspended sediment concentration; P = precipitation; Z_S = tidal elevation; Z_B = bottom elevation; Q = mean discharge; D_S = median size of suspended sediment; D_B = median size of bottom sediment; R_F, R_E = flood and ebb tidal range; MSRRO = Municipal Shenzhen River Regulation Office; MWAB = Municipal Water Affairs Bureau. Refer to Fig. 1 for information of stations.

Survey type	Station	Parameter	Period	Frequency	Data source
Synchronous survey	S1, S2, S3, S5, S7, S11	V, S, C	October 17–18, 2004 October 25–26, 2004 June 16–17, 2005 June 23–24, 2005	Every 30 or 60 min	MSRRO
Continuous survey	LH	P	2007–2009	Daily	MSRRO
		V, C	2007–2009	Every 10 min	
	SZHK	P	2007–2009	Daily	
		V, C	2007–2009	Every 10 min	
	CW	Z_S	2007–2009	Hourly	
Bathymetry survey	River	Z_B	2007–2009	Twice each year	MSRRO
	Bay	Z_B	2007–2009	Once each year	
Historical data	PYHK	P, Q, C, D_S, D_B	1998–2009	Monthly	MSRRO
	CW	P, Z_S, R_F, R_E	1964–2002	Monthly	MWAB

study region. These data were provided by the Municipal Shenzhen River Regulation Office of Shenzhen and Municipal Water Affairs Bureau of Shenzhen in digital data format. Available data included the monthly meteorological and hydrographic data at Ping Yuan He Kou (PYHK, located 13.4 km upstream of the river mouth) from 1998 to 2009 and meteorological and tidal data at CW from 1965 to 2002 (see Table 2). Because both stations were located adjacent to the study region and covered a relatively longer time span, they can be used to study the trends of the driving forces.

3.2. Analysis procedure

3.2.1. Field data analysis

Depth-averaged current velocity, salinity and SSC were calculated from the synchronous survey data measured at different depths. For the continuous survey data, a low-pass digital filter introduced in Wall et al. (2008) was used to separate the tidal signals from those related to processes with longer periods. Because the average tide duration was 12.8 h, a cut-off frequency of 1/26 Hz was selected to filter out signals with periods longer than two consecutive tides. The outputs are low-frequency signals related to processes with long periods (e.g. neap–spring tidal transitions, seasonal transitions, etc.), and the differences between the inputs and outputs are high-frequency signals related to semidiurnal tides and small-scale fluctuations.

Bottom topography can be interpolated from bathymetry data. An average bed elevation was calculated for each cross section of Shenzhen River. For Shenzhen Bay, it is necessary to interpolate the bathymetry data into a two-dimensional computational grid. Grid generation and bathymetry interpolation were accomplished by DELFT-GRID, a pre-processing module of the DELFT model. Interpolated data can be exported for calculating annual bed elevation changes.

The trends of the driving forces during urbanization are of particular interest. However, data at PYHK do not cover the whole period due to data availability. Therefore, we assume that the trends during urbanization are consistent. The Mann–Kendall (MK) test (Mann, 1945; Kendall, 1975) was used to detect possible trends in historical time series with their magnitudes estimated by Sen's approach (Sen, 1968). The MK test is a non-parametric test widely used for trend detection in hydrological studies (Hirsch et al., 1982; Hamed and Ramachandra Rao, 1998; Yue et al., 2002; Zhang et al., 2006). Readers can refer to Hirsch et al. (1982) for detailed analysis procedures.

3.2.2. Numerical analysis

The two-dimensional depth-averaged version of DELFT model (hereafter referred to as 2DH-DELFT model) was used to simulate the hydrological and morphological processes in the estuary. The 2DH-DELFT model uses the coupled depth-averaged shallow water equations and sediment transport equations as the governing equations. To close the sediment transport model, the empirical Partheniades (1965) formula for cohesive materials is adopted to calculate the equilibrium sediment transport rate. Bed elevation changes are calculated with the continuity equation for bottom materials. The interested readers can refer to Lesser et al. (2004) for more details of the 2DH-DELFT model. In the present study, the model was validated with data from the synchronous surveys and the bathymetry surveys. The long-term morphological processes were then simulated under prescribed scenarios to predict the morphological trends and analyze the impact of the driving forces on the estuary.

4. Results

4.1. Synchronous surveys

The ambient conditions, including tidal phase, daily river discharge, water temperature, wind speed and direction, of the four synchronous surveys are listed in Table 3. No significant differences are observed for water temperature, wind speed or wind direction between these surveys. Therefore, the differences in the flow and SSC distributions are primarily caused by tides and river discharge.

4.1.1. Spring-tide (October 17–18, 2004) and neap-tide (October 25–26, 2004) surveys in the dry season

The depth-averaged current velocity, salinity and SSC measured in the first two surveys are plotted in Figs. 2 and 3. These surveys were both conducted in the dry season with very low river discharge, and therefore the current velocity, salinity and SSC distributions of these two surveys were similar. The current velocity profiles in both surveys show regular flood–ebb tidal patterns, indicating dominant tidal controls in the dry season. The peak current velocity was slightly higher in the spring-tide survey (ranging from 0.37 m/s at S1 to 0.71 m/s at S3) than in the neap-tide survey (ranging from 0.28 m/s at S1 to 0.63 m/s at S3). The outer bay (S7 and S11) was occupied by saline seawater (27–28 ppt), the upper tidal channel (S1) was constantly below 2 ppt in the survey, and wide salinity variations were observed for the rest of the stations. It is shown that the upper limit of the salinity intrusion was in the channel between S1 and S2 in the dry season. Inspection of the vertical salinity profiles (not shown) reveals that the estuarine waters were quite homogeneous in salinity. The SSCs were below 0.15 kg/m^3 at all stations, with no clear turbidity maxima observed during the survey.

It is illuminating to examine how SSC varied with current velocity at different stations. The SSCs in the outer bay (S11 and S7) were generally low (0.029–0.086 kg/m^3 in the neap-tide survey, 0.040–0.073 in the spring-tide survey) in both surveys, representing the background SSC levels in the oceanic water at these stations. In the inner bay (S5), the SSC slightly increased with current velocity, which is likely to be caused by local resuspension of deposited materials. The SSC peaks at the river mouth (S3) occurred shortly after the SSC peaks at S5 in flood currents, indicating that the SSC increase at the river mouth is mainly caused by advective sediment transport from the inner bay. The SSC peaks in the upper tidal channel (S1 and S2) occurred in ebb currents in the neap-tide survey and in flood currents in the spring-tide sur-

Table 3
Ambient conditions of synchronous surveys. River discharges are daily average values.

No.	Survey period	Moon phase	River discharge (m^3/s)	Water temperature (°C)	Wind speed (m/s)	Wind direction
1	2004/10/25–2004/10/26	Neap	2.98	26.0	4.1	E
2	2004/10/17–2004/10/18	Spring	2.87	27.3	2.8	NE
3	2005/6/16–2005/6/17	Neap	6.85	28.4	2.7	ENE–E
4	2005/6/23–2005/6/24	Spring	29.1	26.7	2.6	SSE

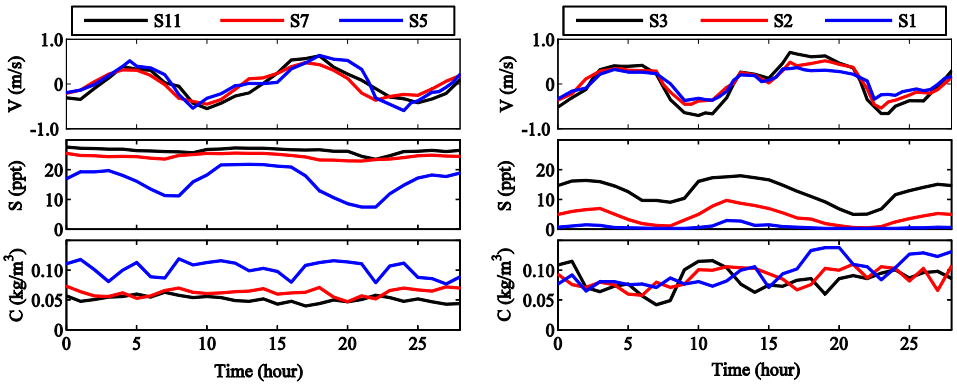

Fig. 2. Current velocity, salinity and suspended sediment concentration time series measured in the first synchronous survey (October 17–18, 2004, neap tides in the dry season) for: S11, S7 and S5 (left); S3, S2 and S1 (right). *V* = current velocity; *S* = salinity; *C* = suspended sediment concentration. Time starts at 11:00 am October 17, 2004.

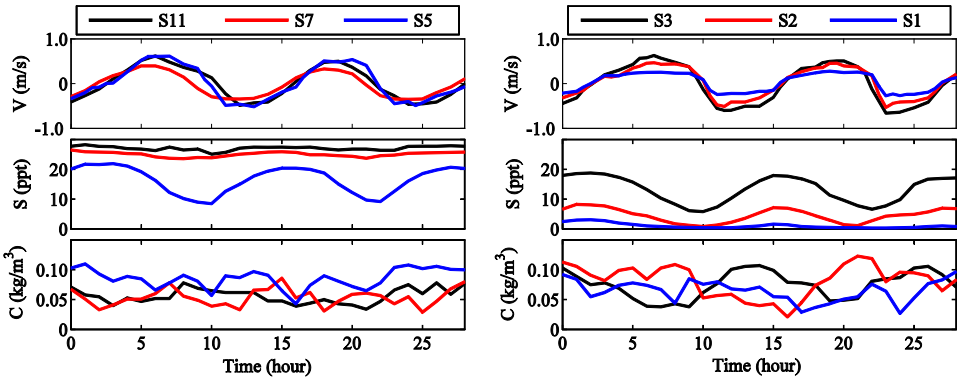

Fig. 3. Current velocity, salinity and suspended sediment concentration time series measured in the second synchronous survey (October 25–26, 2004, spring tides in the dry season) for: S11, S7 and S5 (left); S3, S2 and S1 (right). *V* = current velocity; *S* = salinity; *C* = suspended sediment concentration. Time starts at 6:00 am October 25, 2004.

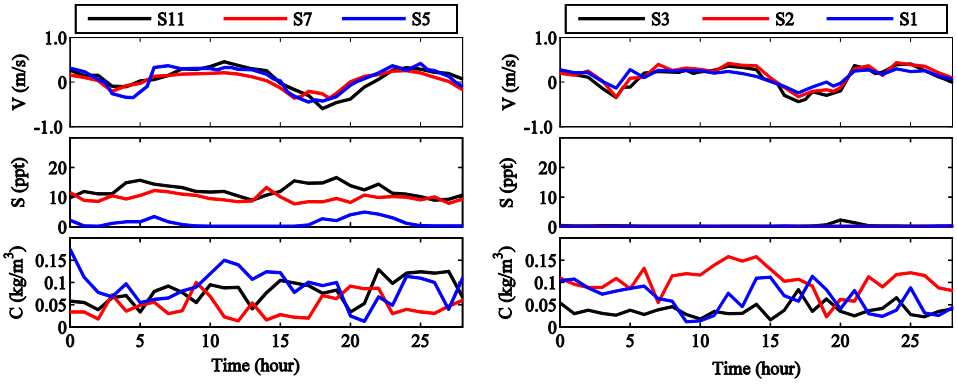

Fig. 4. Current velocity, salinity and suspended sediment concentration time series measured in the third synchronous survey (June 16–17, 2005, neap tides in the wet season) for: S11, S7 and S5 (left); S3, S2 and S1 (right). *V* = current velocity; *S* = salinity; *C* = suspended sediment concentration. Time starts at 10:00 am June 16, 2005.

vey, indicating that they could be affected by sediment from the bay and the upper tributaries.

4.1.2. Spring-tide (June 23–24, 2005) and neap-tide (June 16–17, 2005) surveys in the wet season

The current velocity, salinity and SSC measured in the last two surveys are plotted in Figs. 4 and 5. These surveys were conducted in the wet season with increasing river flow, and therefore can be compared with previous surveys to study the impacts of river discharge on flow and SSC distributions. The ebb current velocity increased with river discharge, ranging from 0.26 m/s at S7 to 0.46 m/s at S11 in the neap-tide survey and 0.57 m/s at S7 to 1.38 m/s at S2 in the spring-tide survey, and the current velocity profiles were distorted toward an ebb-dominated pattern. The upper limit of the saline intrusion moved to the bay between S5 and S7, showing a seaward shift of the estuarine transition zone. In the neap-tide survey with moderate river flow, the river flow was not sufficiently strong to cause any significant changes in the SSC distribution. In the spring-tide survey with high river flow, significant SSC increases were observed at most stations following the current velocity increases. However, the SSC remains relatively low at S7, indicating the existence of a persistent low-SSC region in the central bay despite the different ambient conditions in all surveys.

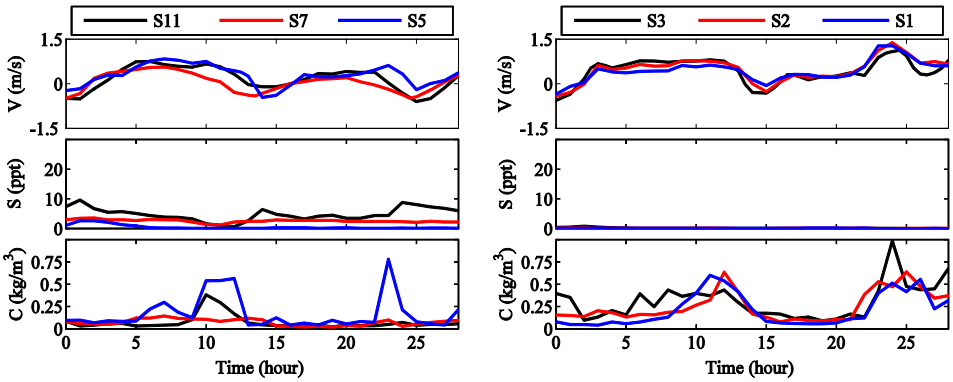

Fig. 5. Current velocity, salinity and suspended sediment concentration time series measured in the fourth synchronous survey (June 23–24, 2005, spring tides in the wet season) for: S11, S7 and S5 (left); S3, S2 and S1 (right). *V* = current velocity; *S* = salinity; *C* = suspended sediment concentration. Time starts at 8:00 am June 23, 2005.

The phase relation between current velocity and SSC in the neap-tide survey is fairly similar to the surveys conducted in the dry season. The SSCs in the river (S1, S2 and S3) showed slight increases in the flood and the ebb tides, indicating they can be affected by sediment from both upstream and downstream. In the spring-tide survey, the SSC in the river and the inner bay (S1–S5) increased sharply following two precipitation events occurring in Hour 9–15 and Hour 22–27, indicating that sediment from upper tributaries became an important sediment source. However, the SSC at S7 did not respond to either of these precipitation events, and the SSC at S11 increased in the first precipitation event but not the second, indicating the SSCs at S7 and S11 were possibly controlled by some other mechanisms.

4.2. Continuous surveys

The SSCs at LH, SZHK and CW from 2007 to 2009 are plotted in Fig. 6. The average precipitation of LH and SZHK is also plotted as an indicator of river flow strength. The multi-year-averaged annual precipitation in Shenzhen is 1905 mm, and annual precipitations from 2007 to 2009 were 1581.5 mm, 2710 mm and 1611 mm, respectively. Therefore, 2007 and 2009 were drier than usual, and 2008 was extremely wet. The SSCs at the three stations were similar in the dry season, but the SSCs at LH and SZHK were generally higher than that at CW in the wet season possibly due to increasing sediment fluxes from upper tributaries. The impact of the seasonal precipitation pattern on SSC was most evident at LH. The SSC at LH consisted of mostly high-frequency signals in the dry season, but was dominated by low-frequency signals during high river discharge in the wet season, indicating that the dominant transport pattern shifts from tidal transport to riverine transport. The impact of the precipitation pattern on SSC is similar but dampened at SZHK and CW possibly due to increasing tidal control. It is noted that the SSCs recorded in 2009 generally decreased at all stations and exhibited almost no response to the precipitation in the wet season.

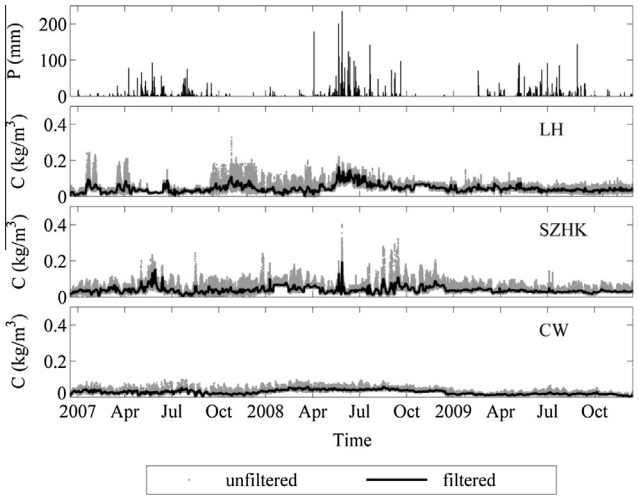

Fig. 6. Precipitation (average of LH and SZHK), suspended load concentration (LH, SZHK and CW) time series recorded from 2007 to 2009. *P* = precipitation; *C* = suspended load concentration; unfiltered = original data sets; filtered = output data from the low-pass digital filter, representing low-frequency components related to non-tidal processes.

The current velocity and SSC time series recorded in two neap–spring cycles at LH, SZHK and CW are presented in Fig. 7–9 (tide elevation at CW is used due to lack of current data). The first neap–spring cycle is in January 2009 with no precipitation (neap tide on January 6 and spring tide on January 13), and the second neap–spring cycle is in June 2008 with intensive precipitation (neap tide on June 12 and spring tide on June 19). The current velocity at LH shows evident flood–ebb tidal patterns in both periods. During the first cycle, the SSC peaks at LH occurred twice each semidiurnal tide during the maximum flood and ebb at spring tides (January 11–14), but occurred only once during the maximum flood for the rest of the neap–spring cycle. At SZHK, the SSC peaks occurred only once during the maximum flood over the whole neap–spring cycle. At CW, the SSC peaks were not completely in phase with tides. In some cases, only one SSC peak was found over two consecutive semidiurnal tides.

Two major precipitation events occurred during the second neap–spring cycle on June 12–14 and 16–18, 2008. Ebb currents were significantly enhanced by increasing river discharge, and the SSC peaks at LH and SZHK were found to occur during ebb currents, indicating that suspended sediment at LH and SZHK was primarily contributed by upper tributaries during precipitation times. After the precipitation events, the SSC peaks were again observed to occur during flood currents, indicating that sediment transport pattern quickly recovered to tidal transport. However, it is noted that the SSC at SZHK was surprisingly low after the precipitation events. The SSC at CW is generally higher than that during the first neap–spring cycle, but show no responses to the two precipitation events, again indicating that the impact of Shenzhen River on the SSC at the outer part of the estuary is rather limited.

4.3. Bathymetry surveys

Only the bathymetry data surveyed in January 2008 (post-flood survey), May 2008 (pre-flood survey), December 2008 (post-flood

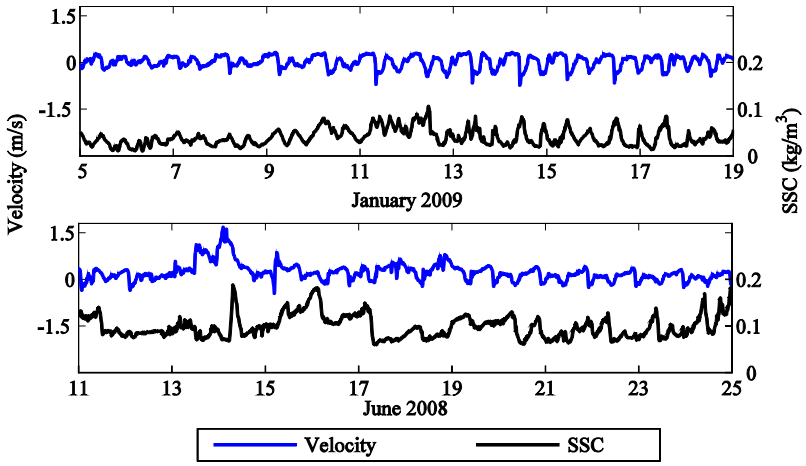

Fig. 7. Current velocity and SSC time series recorded at LH in two neap–spring cycles. Top: January 5–18, 2009; bottom: June 11–24, 2008.

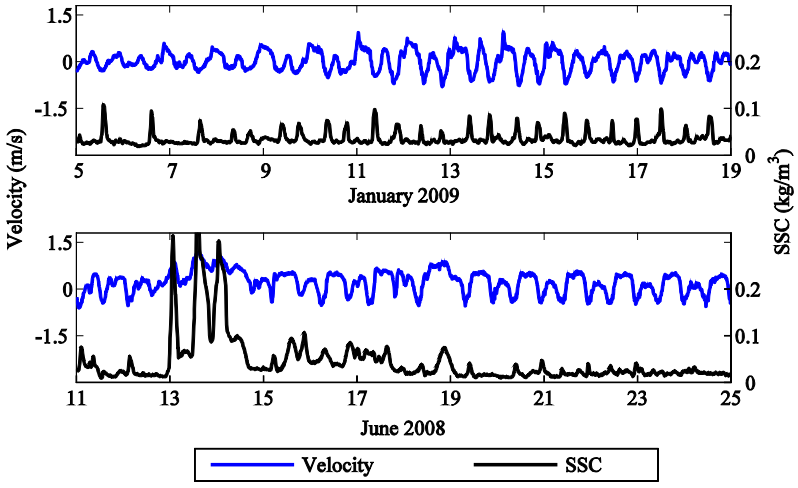

Fig. 8. Current velocity and SSC time series recorded at SZHK in two neap–spring cycles. Top: January 5–18, 2009; bottom: June 11–24, 2008.

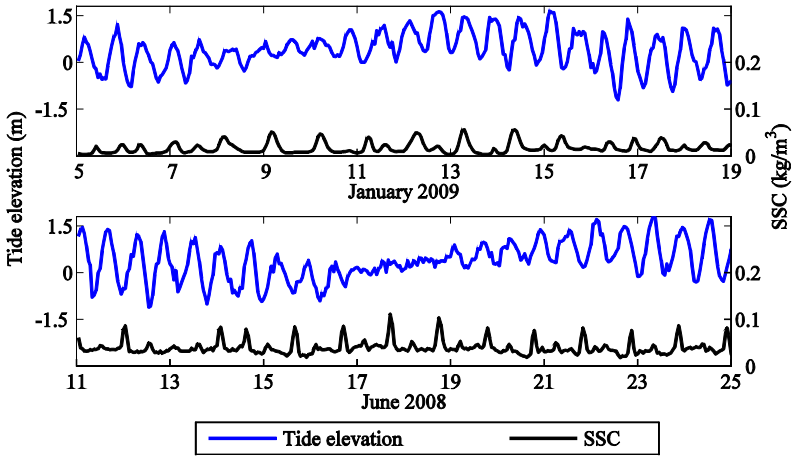

Fig. 9. Tide elevation and SSC time series recorded at CW in two neap–spring cycles. Top: January 5–18, 2009; bottom: June 11–24, 2008. SSC are from the average values of recorded data from two turbidity sensors mounted in the cross section.

survey), April 2009 (pre-flood survey) and December 2009 (post-flood survey) are analyzed in this study for two reasons: (1) the river upstream of LH and the outer bay was not surveyed prior to the survey of January 2008 and (2) dredging activities were performed in the river during 2004 and 2007, which might disturb the bed configuration. Although available bathymetry data are insufficient to corroborative any quantitative conclusions on estuarine morphological processes, it is still helpful to compare the bed

elevation changes occurred in two years with very different precipitation conditions.

4.3.1. Bed elevation changes in Shenzhen River

The bed elevation profiles and the bed elevation changes between two consecutive bathymetry surveys in 2008 and 2009 are plotted in Fig. 10. A total of $\sim 0.51 \times 10^6$ m^3 of sediment was deposited in the channel from January 2008 to December 2009, indicating that the river channel was in a depositional state. Sediment deposition mainly occurred in three sections of the channel: upper section upstream of km 10.0, middle section between km 7.2 and km 4.0, lower section downstream of km 1.0, and remained relatively stable in other sections. The first two sections coincide with the reach where dredging activities were carried out and the channel bed could be far from its equilibrium state, and the last section is near the river mouth. It is also observed that the depositional depth of 2009 was generally higher than that of 2008. Owing to the frequent precipitation in 2008, sediment from upper tributaries was carried much further seaward than in the normal hydrological condition, thereby is less likely to settle in the river. In 2009 with less precipitation, sediment was found to accumulate more upstream. Therefore, it is concluded that the location of sediment deposition is strongly affected by the strength of the river flow.

4.3.2. Bed elevation changes in Shenzhen Bay

Annual bed elevation changes from January 2008 to December 2008 and from Dec 2008 to Dec 2009 are computed from the post-flood bathymetry surveys and plotted in Fig. 11. The time intervals between two consecutive post-flood bathymetry surveys are approximately one year, and therefore can be used to study the annual sedimentation patterns in Shenzhen Bay. General sediment deposition is observed in both years, but is much heavier in 2009 than in 2008 ($\sim 2.2 \times 10^6$ m^3 in 2008 and $\sim 1.8 \times 10^7$ m^3 in 2009). The area with a deposition depth of over 0.3 m included the navigation channel on the north of the bay mouth and a portion of the central outer bay in 2009, which is apparently larger than that in 2008. A large portion of the inner bay also recorded an depositional depth of 0.1–0.3 m in 2009, while almost no sediment deposition was observed in most parts of the inner bay in 2008. Scattered sediment deposits were observed along the submarine channel near the river mouth, but the deposition volume is much smaller than in the outer bay.

4.4. Trend analysis of historical data

Historical time series including the Monthly Total precipitation (MTP) at PYHK and CW, the Mean Discharge (MD) and the Mean Suspended Sediment Concentration (MSSC) at PYHK, the Mean Sea Level (MSL), the Mean Flood Tide Range (MFTR) and the Mean Ebb Tide Range (METR) at CW are analyzed to explore the trends of the driving forces, especially in the urbanization of Shenzhen. Results of the trend analysis are shown in Table 4.

No significant trends are detected in the MTP time series at PYHK. Longer precipitation time series at CW is tested for consistency. Again, no significant trends are detected. The MTP time series is an indicator of precipitation patterns. Therefore, the precipitation can be considered stable in this study. The MD time series shows an upward trend by 0.133 m^3/s per year. The positive trend of the MD time series is possibly an outcome of increasing built-up areas in the catchment of Shenzhen River. Ng et al. (2011) reported that the urban built-up area in Shenzhen sharply increased from 22.71 km^2 in 1988 to 140.10 km^2 in 2008. Increasing surface runoff generation usually results in more severe soil erosion in the catchment (Van Rompaey et al., 2002). However, the MSSC is observed to slightly decrease during the study period. From Table 2 in Ng et al., 2011, it is shown that the total fraction of Forest and Yuan land (orchard land) was almost unchanged from 1988 to 2008, and the increase of the urban built-up areas was mainly from cultivated land, a land use type that is highly susceptible to soil erosion under heavy rainfall. Therefore, it should be concluded that the slightly decreasing MSSC is a combined effect of the increase of urban built-up area and the well-kept forest and orchard land.

For the tidal time series of CW, the MSL time series shows an upward trend by 1.96 mm per year, which agrees with the estimated value of 1.8–2.0 mm per year for the Pearl River estuary for the last 50 years (Zhang et al., 2010). Meanwhile, no significant trends are detected for both the MFTR and METR time series, which seems to contradict with the results of Zhang et al. (2010). Zhang et al. (2010) analyzed tidal series at 17 gauges in the Pearl River estuary, and found that the gauges near the estuary showed negative trends for tidal ranges during the study period. They also suggested that the change of flood range is possibly caused by human activities rather than natural impacts. If we divide the MFTR and METR time series of CW into two sub-series, one from 1964 to 1980 (representing the pre-urbanization period) and the other from 1981 to 2002 (representing the urbanization period), negative trends are detected for the tidal range during urbanization period by 2.3–2.4 mm per year, which matches the values at the river mouth stations (1.2–5 mm per year for Hengmen, Wanqingsha and Nansha) in the study of Zhang et al. (2010). Therefore, the tidal force of the estuary is concluded to be decreasing during the urbanization of Shenzhen.

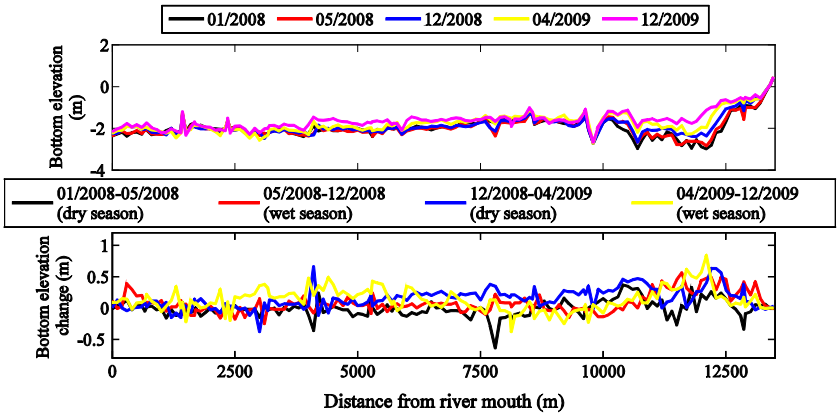

Fig. 10. Measured average bed elevation profiles (upper) and bed elevation changes (lower) between two consecutive bathymetric surveys in the Shenzhen River. Local Shenzhen River reference coordinates are used in all bathymetric surveys. Bottom elevation changes are computed as the differences between the bed elevation profiles measured in two consecutive bathymetric surveys. Figure legends denote the dates of the bathymetric surveys.

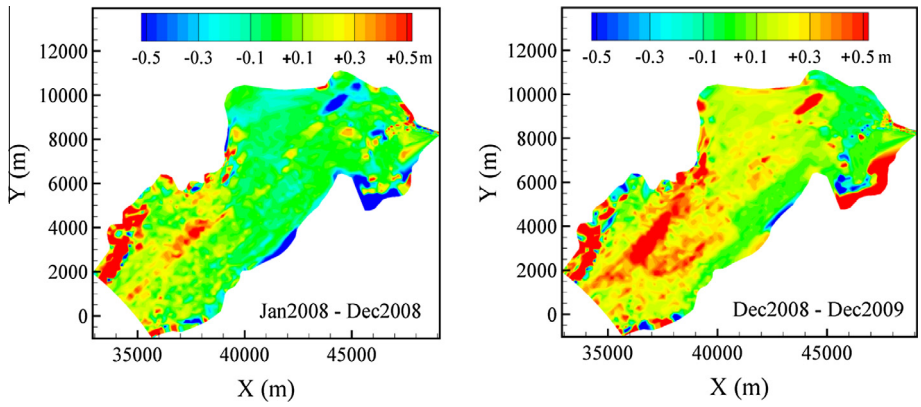

Fig. 11. Bed elevation changes of Shenzhen Bay from January 2008 to December 2008 (left) and from December 2008 to December 2009 (right). Bed elevation changes are computed as the differences between the bed elevation profiles measured in two consecutive bathymetric surveys. Positive values in the scale bar indicate sediment deposition.

Table 4
Results of MK test at PYHK and CW. MTP = monthly total precipitation; MD = mean discharge; MSSC = mean suspended sediment concentration; MSL = mean sea level; MFTR = mean flood tide range; METR = mean ebb tide range.

Parameter	95% Significant?	Trend	Sen's slope
MTP at PYHK (1998–2009)	No	–	–
MTP at CW (1965–2002)	No	–	–
MD at PYHK (1998–2009)	Yes	Increasing	1.33×10^{-1} m^3/s/year
MSSC at PYHK (1998–2009)	Yes	Decreasing	-5.38×10^{-3} kg/m^3/year
MSL at CW (1964–2002)	Yes	Increasing	1.96×10^{-3} m/year
MFTR at CW (1964–2002)	No	–	–
METR at CW (1964–2002)	No	–	–
MFTR at CW (1981–2002)	Yes	Decreasing	-2.35×10^{-3} m/year
METR at CW (1981–2002)	Yes	Decreasing	-2.26×10^{-3} m/year

4.5. Numerical analysis

4.5.1. Model setup and validation

The synchronous surveys are used to test the validity of the flow module of the 2DH-DELFT model. The computational domain consists of the main stream of Shenzhen River from SZHK to PYHK and Shenzhen Bay. Bathymetry data from the 2007 post-flood survey are used to generate the bottom geometry. The water level, salinity and SSC time series of CW are used to generate boundary conditions for the bay mouth. River flow from tributaries was treated as side flow in the model. Uniform distributions of water level, salinity and sediment concentration are used as initial conditions. A "warm-up" period of approximately 20 tides is used to eliminate the impact of inaccurate initial conditions. Two types of particles are used to represent the sediment mixture: the coarser particles with a settling velocity of 0.2 mm/s (corresponding to a grain size of ~20 μm) and the finer particles with a settling velocity of 0.03 mm/s (corresponding to a grain size of ~7 μm). A Manning's roughness coefficient of 0.03 was used. The erosional parameter and the erosional shear stress are calibrated to match the survey data. A time step of 0.5 min is used in all simulations.

The computed current speed, salinity and SSC at S7 and S3 are compared with the survey data in Fig. 12. The computed current speed matches the measured data very well during the dry season, but is slightly underestimated in the wet season possibly because the surface runoff directly flowing into the bay is not accounted for in the model. Similarly, the simulated salinity matches well with the measured data in the dry season, but is less accurate in the wet season due to the underestimated surface runoff. The simulated SSC are of similar magnitudes with the measured data, although some small fluctuations cannot be accurately reproduced. In general, the simulated results are in reasonable agreements with

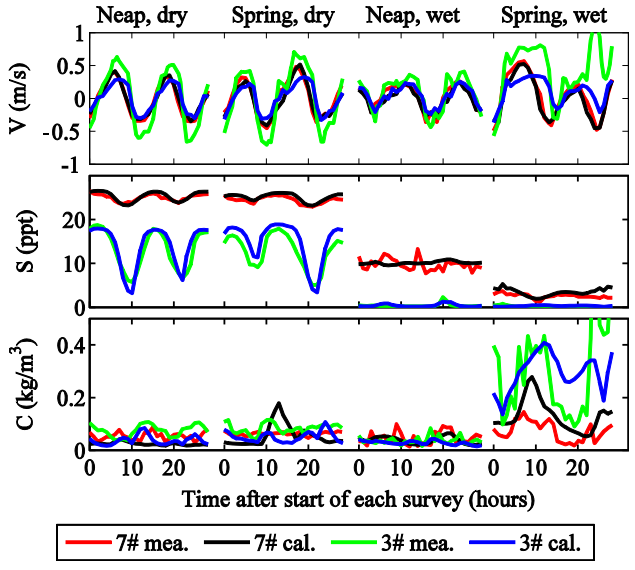

Fig. 12. Comparison of simulated and measured current velocity, salinity and suspended sediment concentration at S7 and S3 in the four synchronous surveys. *V* = current velocity; *S* = salinity; *C* = suspended sediment concentration.

the measured data, which justifies the use of the 2DH-DELFT model in simulating the flow and sediment transport in the estuary.

Sediment transport and the consequential morphological processes in 2008 and 2009 are simulated to validate the morphological module of the 2DH-DELFT model. The tide elevation and the SSC time series at CW from the continuous surveys are used as boundaries conditions for the bay mouth. River discharge and

SSC at PYHK are used as side flow boundaries. For other tributaries where the discharge and SSC data are not available, the flow boundaries are interpolated from the survey data of PYHK based on their catchment areas, and the SSC boundaries are simply assumed the same as in PYHK. Other computational parameters are calibrated to achieve a better match with the actual bed elevation changes.

The spatial distributions of the simulated bed elevation changes in 2008 and 2009 are plotted in Fig. 13. There are several aspects that the simulated results agree with the observation: (1) sediment deposition mainly occurs in the in the outer bay near the bay mouth; (2) very light deposition and erosion is observed in most area of the inner bay (except a small area near the submarine channel in the simulation), with scattered sediment deposits observed near the river mouth; and (3) sediment deposition in the outer bay is much stronger in 2009 than 2008. This indicates that the numerical model captures some key features of sedimentation in the bay. However, there is an apparent discrepancy between the simulated and the observed bed elevation changes: the model shows strong erosion in a narrow channel situated in the center of the bay, in both simulated situations of 2008 and 2009. However, these changes are not visible in Fig. 11, where net accretion is measured especially in 2009. The sedimentation volumes predicted by the model are 2.27×10^6 and 9.55×10^6 m^3 in 2008 and 2009 respectively, comparing the observed values of 2.23×10^6 and 17.70×10^6 m^3. There are several possible reasons for the discrepancy between the simulated and observed spatial sedimentation patterns and deposited volumes in the bay: (1) the sedimentation process of fine cohesive particles are affected by their size distribution, layer structure, stress history, biochemical composition and other factors, and thus cannot be well described by the empirical Partheniades (1965) formula which computes the sediment transport flux based on a critical shear stress and an erosional constant and (2) sedimentation in the Shenzhen River estuary is strongly disturbed by frequent extreme events such as subtropical cyclones and rainstorms, which are not accounted for in the model. For example, Typhoon Hagupit in 2008 and Molave in 2009 induced more than 1 m storm surge in the area, which might generate a certain deposition. The model results may be potentially improved by implementing more sophisticated modules with tunable parameters. However, such a plausible solution may allow too many degrees of freedom and thus impair the model credibility. Because the simulated spatial sedimentation pattern roughly matches the observed one (except in near the submarine river zone), we will assess the spatial pattern in the estuarine sedimentation processes with the model, but remain cautious about the quantitative simulation results.

4.5.2. Simulated current velocity, salinity and SSC fields during the maximum floods and ebbs

The simulated distributions of current velocity, salinity and SSC during maximum floods and ebbs in the two spring-tide synchronous surveys are plotted in Fig. 14. River discharge shows a substantial impact on estuarine flow, resulting in weaker flood currents and stronger ebb currents in the wet season. The flood current velocity in the navigation channel on the north side of CW is significantly larger than its south side, forming the main entrance for marine water and suspended sediment from the Pearl River estuary. The ebb current velocity is more uniform over the cross section. This is consistent with the observation that sediment deposition is more severe on the north side than the south side near the bay mouth. In the inner bay, flow is stronger in the submarine channel than in the mudflats in the wet season due to increasing river discharge. The SSC levels near the bay mouth and the river mouth are separated by a persistent low-SSC zone at the central bay in the dry season, whereas in the wet season the high-SSC zone near the river mouth extends to the central bay and connects with the high-SSC zone near the bay mouth due to increasing riverine sediment supply.

4.5.3. Residual fields of sediment transport of 2008 and 2009

The residual fields of SSC and suspended sediment transport rate of 2008 and 2009 were plotted in Fig. 15. The residual SSC level is higher in the inner bay than in the outer bay in 2008, whereas the opposite is observed in 2009. This indicates the different contributions to the suspended sediment in the bay by marine sediment transport and riverine sediment transport for the two years due to varying stream volumes. It is also shown that the residual SSC level in the outer bay is generally higher in 2009 with low river flow than in 2008 with very high river flow. This is consistent with the morphological pattern shown in Fig. 11, where deep intrusion of sediment deposition is found to concur with decreasing river flow. The importance of river flow in the morphological process of the estuary is confirmed by the residual sediment fields from the simulation.

4.5.4. Long-term simulation of the morphological processes in Shenzhen Bay

A numerical simulation is carried out using the 2DH-DELFT model to evaluate the long-term morphological changes in Shenzhen Bay. At the present stage, we assume the driving forces of the estuarine flow and sediment transport are stable in the annual scale. Therefore, the boundary conditions for the long-term simulation can be generated with the survey data of 2008 and 2009. The flow boundary for the bay mouth is prescribed with the tide

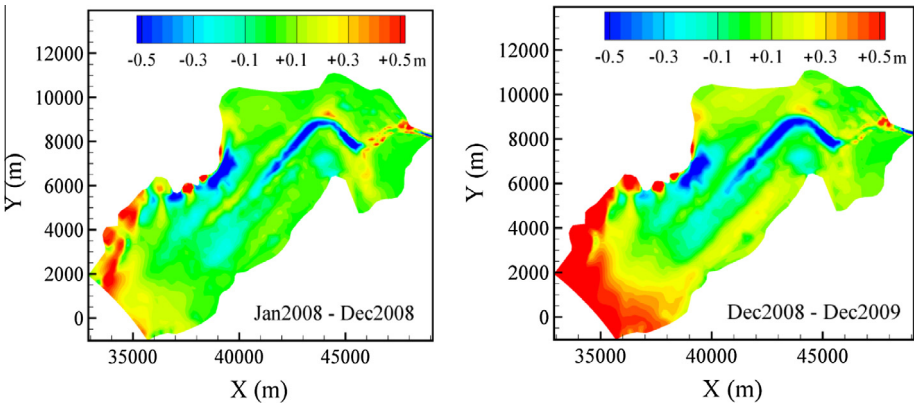

Fig. 13. Simulated bed elevation changes of Shenzhen Bay from January 2008 to December 2008 (left) and from December 2008 to December 2009 (right). Values are bed elevation differences computed with exported bed elevation profiles from the DELFT-FLOW model for specific dates.

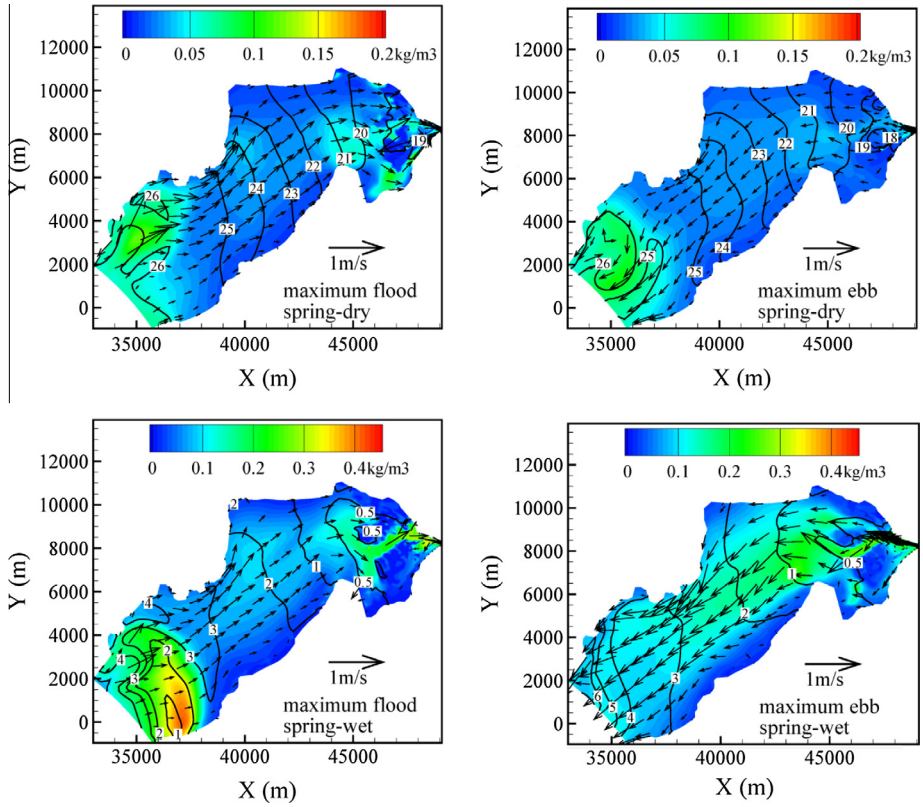

Fig. 14. Simulated spatial distributions of current velocity (vectors), salinity (contour lines) and SSC (color contours) during maximum flood (upper-left, occurring at 20:00, October 17 of 2004), maximum ebb (upper-right, occurring at 15:00, October 17 of 2004) of spring tides in the dry season and during maximum flood (lower-left, 22:00, June 23 of 2005), maximum ebb (lower-right, 15:00, June 23 of 2005) of spring tides in the wet season. (For interpretation of the references to color in this figure legend, the reader is referred to the web version of this article.)

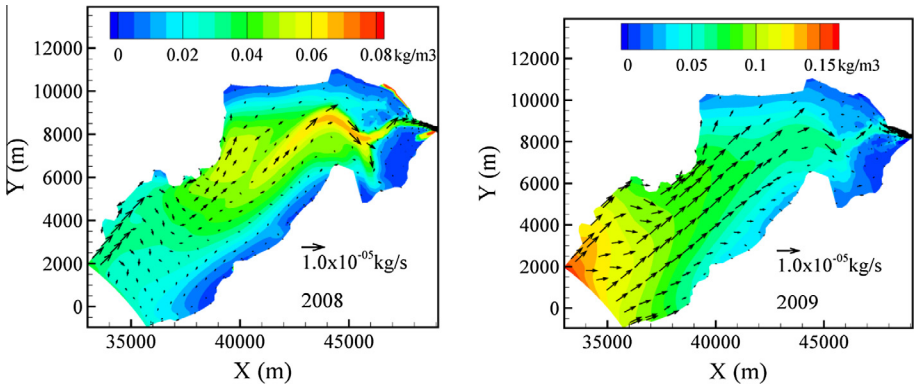

Fig. 15. Simulated residual fields of suspended sediment transport rate (vectors) and SSC (color contours) for 2008 (left) and 2009 (right). Residual fields are obtained from annually averaged suspended sediment transport rate and SSC fields. (For interpretation of the references to color in this figure legend, the reader is referred to the web version of this article.)

elevation time series at CW generated by tidal harmonic analysis to eliminate the impact of extreme events. For other boundary conditions, the original survey data are used. The 2DH-DELFT model provides a computational parameter called "morphological scale factor", by which the simulated bed elevation changes are amplified at each time step. In the present study, the simulation period is two years and the morphological scale factor is selected as 25, equivalent to the morphological process occurring in 50 years.

The simulated bed elevation changes of Shenzhen Bay are shown in Fig. 16. It is shown that general deposition occurs over the inner bay and along the coastlines on both sides of the outer bay where the water depth is relatively smaller, and erosion occurs along the center line from submarine channel to the outer bay. The deposition depth is mostly between 0 and 2 m, but can be over 3 m near the river mouth and along the north coastline of the outer bay. Under such circumstances, Shenzhen Bay gradually shrinks and becomes part of the channel.

4.5.5. Long-term morphological responses to the trends of driving forces

Long-term simulations show the possible sediment deposition pattern in the next few decades with current ambient conditions. However, the simulation is performed under the assumption of "stationary driving forces". The trend analysis of the historical time

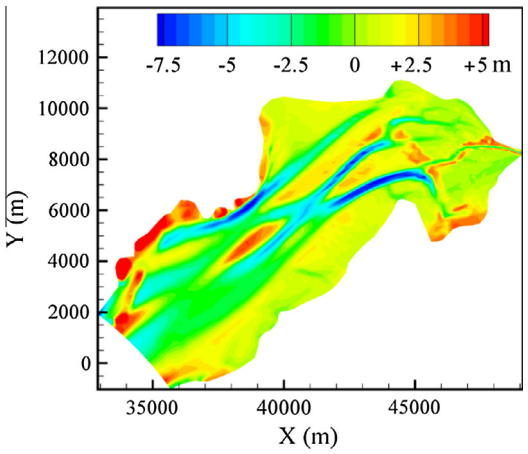

Fig. 16. Simulated bed elevation changes in 50 years using current ambient conditions as the boundary conditions.

series exhibits certain trends of the driving forces. It would be useful to assess how long-term morphological processes will respond to such trends. Therefore, two additional long-term simulations of the morphological process are performed with the current trends of the driving forces: the first scenario assumed a varying sea boundary at CW with elevating sea level and attenuating tidal range, and the second scenario assumed a varying river inflow boundary with increasing river discharges. The river discharges at all tributaries and the sea level and the tidal range at CW 50 years later are computed with the annual rates computed in the trend analysis. The river discharge and the tidal range are determined to be 2.5 and 0.8 times their current values, respectively. The global sea level rise is estimated to be 0.1 m. The boundary time series are then generated by linear temporal interpolation between the current condition and the future condition. Other parameters are kept the same as used in the long-term simulation reported in Section 4.5.4.

The simulated bed elevation changes are plotted in Fig. 17, which can be compared with the simulated results in the "stationary driving forces" scenario shown in Fig. 16. It is shown that the assumed trends of driving forces in the two scenarios accelerate the deposition process. In the first scenario, the erosion in the center of the outer bay is less severe than in the "stationary driving forces" scenario. In the second scenario, the increasing river discharge causes a more severe deposition especially in the inner bay. This can be confirmed by the sediment deposition volumes computed from the bed elevation changes. Under the two scenarios with varying driving forces, the sediment deposition volumes are $24.90 \times 10^6\ m^3$ and $28.90 \times 10^6\ m^3$, comparing to $7.84 \times 10^6\ m^3$ in the "stationary driving forces" scenario.

5. Discussion

The SSC distribution in an estuary is often characterized by the existence of a turbidity maximum in the estuarine transition zone. According to the model results of a conceptualized estuary in Festa and Hansen (1978), the mixing of tidal flow and river flow creates a stagnation point, where the suspended sediment in the bottom layer is transported to the surface layer to produce an estuarine turbidity maximum slightly seaward of the stagnation point. However, field evidence suggests the absence of a stable turbidity maximum in the Shenzhen River estuary. On the contrary, a low-SSC zone persists near the central bay (S7) for most time of the year. This is not surprising for the dry season, because the SSCs at all survey stations remains low due to weak sediment supplies from both the tidal and riverine transport with low current strengths. When the SSCs in both the Pearl River and Shenzhen River increase with enhanced flow, it is surprising to notice that the SSC at the central bay (S7) remains unchanged. This suggests that the sediment circulation in the estuary is different from the model results computed from the nongravitational circulation theory in Festa and Hansen (1978).

The SSC distribution is possibly related to the stratification of the estuarine water. In a well-mixed or weakly stratified estuary, the upward sediment flux is quickly dissipated. Simpson et al. (1990) proposed to use the Simpson number to indicate the ratio of turbulent kinetic energy to the potential energy change due to tidal straining, which can be expressed as:

$$S_i = b_x H^2 / \left(C_D U_T^2 \right) \tag{2}$$

where S_i is the Simpson Number; $b_x = \beta g s_x$ is the along-estuary buoyancy gradient, $\beta = 7.7 \times 10^{-4}$ is the haline contractility and s_x is the horizontal saline gradient; H = water depth; $C_D = 2.0 \times 10^{-3}$ is the drag coefficient; U_T is the depth-averaged tidal velocity. Stacey and Ralston (2005) suggested that when $S_i < 0.2$ full water-column mixing can occur in both the flood and ebb tides. Assuming constant values of $H = 2.9$ m and $U_T = 0.4$ m/s, the S_i computed using salinity observations in the four synchronous surveys ranges from 0.067 to 0.198, indicating that the estuary is in well-mixed state for most time of the year. Geyer (2010) also proposed to classify the estuaries into weakly stratified and strongly stratified estuaries based on the forcing conditions. He suggested to use the dimensionless freshwater velocity $\overline{u_R}$ and tidal velocity $\overline{u_T}$ as the master variables, which can be defined as:

$$\overline{u_R} = u_R / (\beta g s_o H)^{1/2} \tag{3}$$

$$\overline{u_T} = u_T / (\beta g s_o H)^{1/2} \tag{4}$$

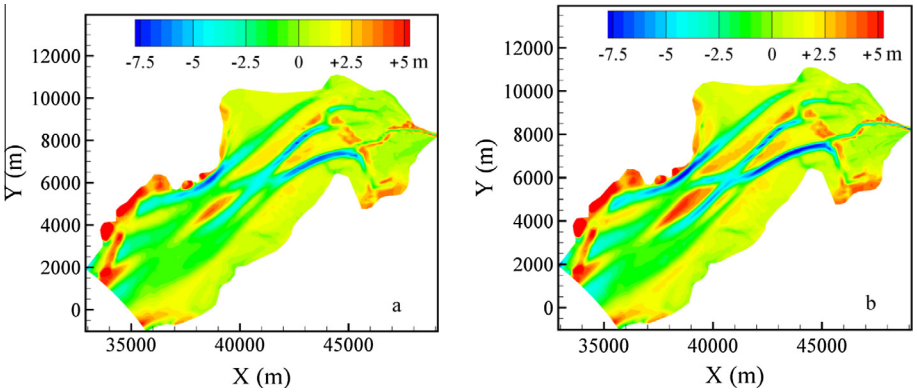

Fig. 17. Simulated bed elevation changes in 50 years assuming: (a) rising sea level and attenuating tidal range at CW (left) and (b) increasing river discharge (right).

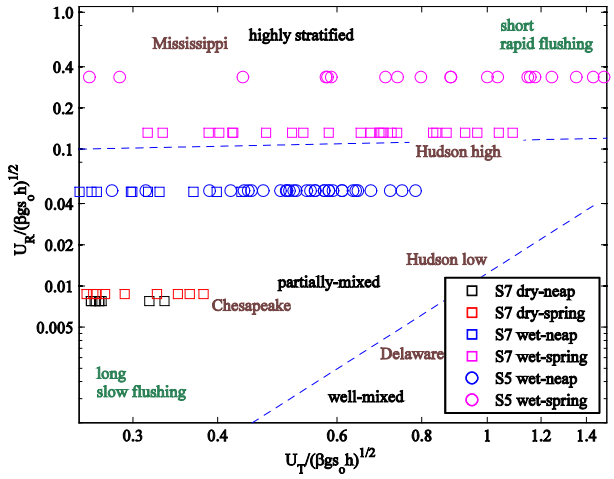

Fig. 18. Prognostic estuarine classification for the Shenzhen River estuary based on Geyer (2010). The x and y axis are dimensionless river velocity and tidal velocity. Values are calculated based on synchronous surveys. Classification of the estuaries except for the Shenzhen River estuary and the locations of classification lines (blue dash lines) are mapped from Fig. 2.7 of Geyer (2010). (For interpretation of the references to color in this figure legend, the reader is referred to the web version of this article.)

where u_R and u_T are freshwater and tidal velocity, respectively; s_o are the oceanic salinity. Then the forcing conditions can be mapped into the $\overline{u_R} - \overline{u_T}$ parameter space. The parameter space for the Shenzhen River estuary is plotted in Fig. 18 with data collected at S7 (representing outer bay) and S5 (representing inner bay) in the four synchronous surveys. The Shenzhen River estuary is classified as a partially mixed estuary in the dry season, but tends to shift to a highly stratified state according to the classification of Geyer (2010). However, the geometry effect is not yet accounted for in the theoretical framework of Geyer (2010). Due to the small water depth of the Shenzhen River estuary, estuarine flow is frequently disturbed by topographic irregularities and small-scale turbulence. As a result, the spatial SSC distribution in the estuary is characterized by its horizontal structure rather than its vertical structure.

The existence of the low-SSC zone suggests that the SSC field in the estuary can be separated into two different systems with low mass exchange: the inner bay and the river form a relatively closed system under the influence of the riverine sediment from upper tributaries ("fluvial zone"), whereas the outer bay is under the influence of marine sediment from the Pearl River estuary ("tidal zone"). Sediment transport in the fluvial zone is characterized by the seasonal shifts of the transport direction: sediment from upper tributaries is carried into the bay during high flow events in the wet season and transported back into the river in the dry season. The phase relation between currents and the SSC within the fluvial zone could be an evidence of the proposed sediment circulation pattern. The seasonal shifts of the sediment transport directions can be also seen in the continuous surveys at LH and SZHK. We calculated the daily and cumulative sediment transport volume from 2007 to 2009 at SZHK (Fig. 19), and found that the landward transport volume in the dry season is approximately equal to the seaward transport volume in the wet season, indicating that the suspended sediment is roving within the system for a long time.

The sediment deposition pattern observed also seems to support the hypothesized sediment circulation pattern. Sediment deposition originated from marine sediment and riverine sediment can be clearly distinguished in Fig. 11, where the two heavily deposited zones are separated by a stable zone with very minor bed elevation changes. This is also consistent with the findings of an geophysical survey by the Municipal Shenzhen River Regulation Office of Shenzhen in 2004 (unpublished data). A total of 55 sediment cores were collected during the survey. Gravel and gravel-sand layer were identified below the surface mud layer in the core samples collected in the samples collected in the inner bay near the river mouth, but not observed in the outer bay samples. Therefore, they concluded that the outer bay and the inner bay were likely to be from different sources.

Finally, the long-term numerical simulations carried out in this study provides some insights into the morphological trends of the Shenzhen River estuary in the future. Although the quantitative results can be highly inaccurate, the accelerating depositional process and the decreasing estuarine capacity are likely to occur. This is already confirmed by observations in existing studies. According to Wang and Chen (2001), the annual deposition rate of Shenzhen Bay has already increased from 16.9 mm per year in 1907–1947 to 30.0 mm per year in 1990–2008. If the trends of the driving forces are to persist in the urbanization, the sediment deposition issue of the Shenzhen River estuary will continue to be aggravated.

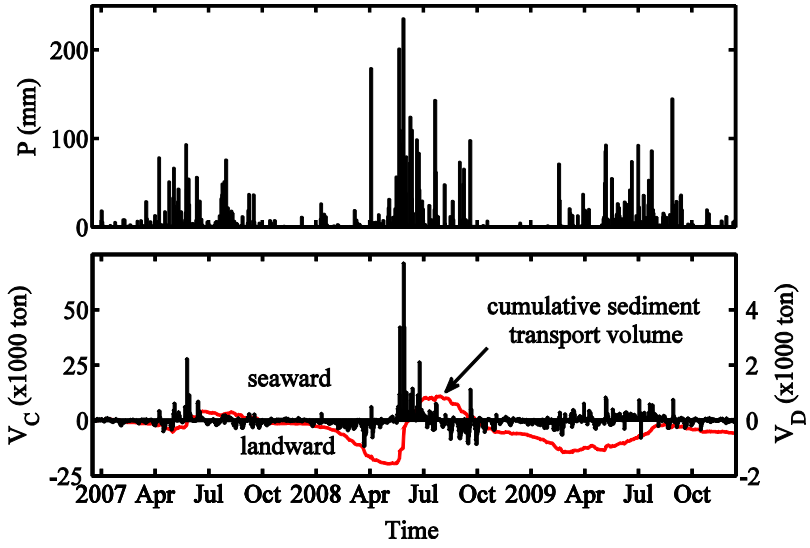

Fig. 19. Daily precipitation, daily and cumulative sediment transport volumes from 2007 to 2009 at SZHK. V_C = cumulative sediment transport volume; V_D = daily sediment transport volume.

6. Conclusions

Due to the geographical importance of the Shenzhen River estuary, heavy sediment deposition becomes a major environmental threat for both Shenzhen and Hong Kong. The hydrographic and bathymetry data have been acquired from the field surveys carried out between 2004 and 2009, which were used to study the flow, sediment circulation and morphological trends of the Shenzhen River estuary. Longer historical time series were also analyzed to detect possible long-term trends in the driving forces of the estuarine circulation. The impacts of the driving forces were then evaluated with the 2DH-DELFT numerical model.

The synchronous surveys show general SSC increases from the dry season to the wet season at most survey stations due to enhanced river flow. However, a persistent low-SSC region is observed near the central bay, thus limiting the sediment mass exchange between the inner bay and the outer bay. Owing its presence, the sediment circulation in the estuary can be separated into two different systems: the SSC in the tidal zone is associated with marine sediment transport in the Pearl River estuary, whereas in the fluvial zone it is primarily contributed by terrestrial sediment from upper tributaries. The locations of the tidal zone and the fluvial zone may vary depending on the strengths of tidal flow and river flow. Increasing river flow can cause the fluvial zone to shift in the seaward direction, resulting in increasing mass exchange between the fluvial zone and the tidal zone. This hypothesized sediment circulation pattern is consistent with the sedimentation patterns revealed by the bathymetry data. The simulated results from the 2DH-DELFT model also exhibit significant differences between the flow and SSC fields in different seasons, confirming the strong impact of the river discharge on estuarine circulation pattern. The proposed estuarine circulation pattern may also apply to other small estuaries with similar settings as the Shenzhen River estuary.

Long-term trends are detected in the hydrographic time series at PYHK and the tidal time series at CW, indicating possible changes in the driving forces during the urbanization of Shenzhen. The river discharge time series show upward trends when the precipitation remains stable, which is possibly caused by the increasing impervious land surface in the catchment. Trends are also detected for the mean sea level and the tidal range time series at CW, which may relate to the intense human activities during urbanization. The impacts of the driving forces on morphological process are assessed under two selected scenarios. In the varying driving force scenario, Shenzhen Bay is shrinking faster than in the stationary driving forces scenario, indicating that human activities in urbanization will further aggravated the already severe sediment deposition in the Shenzhen River estuary. It is advisable to review the development scheme and control the intensity of human activities in order to maintain the ecological environment of the Shenzhen River estuary during its urbanization.

Acknowledgements

This study was supported by China Postdoctoral Science Foundation (2012M510031, 2013T60123), Shenzhen Science and Technology Plan project of China (JCYJ20140902110354253), and Shenzhen Key Laboratory for Coastal Ocean Dynamic and Environment (ZDSY20130402163735964), Graduate School at Shenzhen, Tsinghua University, China. The authors would like to thank the Municipal Shenzhen River Regulation Office and Municipal Water Affairs Bureau of Shenzhen for providing the hydrological, tidal and bathymetric data from the field survey. The tidal data at TBT was provided by the Hong Kong Observatory. We thank Professor John Huthnance at National Oceanography Center, UK, and Professor Zengcui Han at Zhejiang Institute of Hydraulics and Estuary, China for their insightful comments and suggestions in improving the quality of this manuscript. We also thank the editors and anonymous reviewers for their valuable criticisms and suggestions.

References

Burchard, H., Hetland, R.D., 2010. Quantifying the contributions of tidal straining and gravitational circulation to residual circulation in periodically stratified tidal estuaries. J. Phys. Oceanogr. 40, 1243–1262.
Cao, Z., Day, R., Egashira, S., 2002. Coupled and decoupled numerical modeling of flow and morphological evolution in Alluvial Rivers. J. Hydraul. Eng. 128 (3), 306–321.
Carling, P.A., 1982. Temporal and spatial variation in intertidal sedimentation rates. Sedimentology 29 (1), 17–23.
Cayocca, F., 2001. Long term morphological modeling of a tidal inlet: the Arcachon Basin, France. Coast. Eng. 42 (2), 115–142.
Chan, S.N., Lee, J.H., 2010. Impact of river training on the hydraulics of Shenzhen river. J. Hydro-Environ. Res. 4 (3), 211–223.
Chen, S.N., Geyer, W.R., Sherwood, C.R., Ralston, D.K., 2010. Sediment transport and deposition on a river-dominated tidal flat: an idealized model study. J. Geophys. Res. 115 (C10), C10040.
Dastgheib, A., Roelvink, J.A., Wang, Z.B., 2008. Long-term process-based morphological modeling of the Marsdiep Tidal Basin. Mar. Geol. 256 (1), 90–100.
El kadi Abderrezzak, K., Paquier, A., 2009. One-dimensional numerical modeling of sediment transport and bed deformation in open channels. Water Resour. Res. 45 (5), W05404.
Fenster, M.S., FitzGerald, D.M., 1996. Morphodynamics, stratigraphy, and sediment transport patterns of the Kennebec River estuary, Maine, USA. Sediment. Geol. 107 (1), 99–120.
Festa, J.F., Hansen, D.V., 1978. Turbidity maxima in partially mixed estuaries: a two-dimensional numerical model. Estuar. Coast. Mar. Sci. 7 (4), 347–359.
Geyer, W.R., 2010. Estuarine salinity structure and circulation. In: Valle-Levinson, A. (Ed.), Contemporary Issues in Estuarine Physics. Cambridge University Press, Cambridge, pp. 12–27.
Geyer, W.R., MacCready, P.M., 2014. The estuarine circulation. Annu. Rev. Fluid Mech. 46, 175–197.
Hamed, K., Ramachandra Rao, A., 1998. A modified Mann–Kendall trend test for autocorrelated data. J. Hydrol. 204 (1–4), 182–196.
Harris, P.T., Collins, M.B., 1984. Bedform distributions and sediment transport paths in the Bristol Channel and Severn Estuary, UK. Mar. Geol. 62 (1), 153–166.
Hirsch, R.M., Slack, J.R., Smith, R.A., 1982. Techniques of trend analysis for monthly water quality data. Water Resour. Res. 18 (1), 107–121.
Kendall, M.G., 1975. Rank Correlation Methods. Charles Griffin, London, UK.
Lerczak, J.A., Geyer, W.R., 2004. Modeling the lateral circulation in straight, stratified estuaries. J. Phys. Oceanogr. 34, 1410–1428.
Lesser, G.R., Roelvink, J.A., Van Kester, J.A.T.M., Stelling, G.S., 2004. Development and validation of a three-dimensional morphological model. Coast. Eng. 51 (8), 883–915.
Mann, H.B., 1945. Nonparametric tests against trend. Econom.: J. Econom. Soc. 13, 245–259.
Mariotti, G., Fagherazzi, S., 2010. A numerical model for the coupled long-term evolution of salt marshes and tidal flats. J. Geophys. Res.: Earth Surf. 115 (F1), F01004.
National Bureau of Statistics of China (NBSC), 2012. Shenzhen Statistical Yearbook 2012. China Statistics Press, Beijing, China. ISBN: 978-7-5037-6597-1.
Ng, C.N., Xie, Y.J., Yu, X.J., 2011. Measuring the spatio-temporal variation of habitat isolation due to rapid urbanization: a case study of the Shenzhen River cross-boundary catchment, China. Landscape Urban Plann. 103 (1), 44–54.
Partheniades, E., 1965. Erosion and deposition of cohesive soils. J. Hydraul. Div. – ASCE 91 (1), 105–139.
Postma, H., 1967. Sediment transport and sedimentation in the estuarine environment. In: Estuaries. AAAS Publication No. 83, pp. 158–179.
Ralston, D.K., Geyer, W.R., Warner, J.C., 2012. Bathymetric controls on sediment transport in the Hudson River estuary: lateral asymmetry and frontal trapping. J. Geophys. Res. 117, C10013.
Sen, P.K., 1968. Estimates of the regression coefficient based on Kendall's tau. J. Am. Stat. Assoc. 63 (324), 1379–1389.
Seybold, H.J., Molnar, P., Singer, H.M., Andrade Jr., J.S., Herrmann, H.J., Kinzelbach, W., 2009. Simulation of birdfoot delta formation with application to the Mississippi Delta. J. Geophys. Res. 114 (F3), F03012.
Simpson, J.H., Brown, J., Matthews, J., Allen, G., 1990. Tidal straining, density currents, and stirring in the control of estuarine stratification. Estuaries 13, 125–132.
Stacey, M.T., Ralston, D.K., 2005. The scaling and structure of the estuarine bottom boundary layer. J. Phys. Oceanogr. 35, 55–71.
Stacey, M.T., Burau, J.R., Monismith, S.G., 2001. Creation of residual flows in a partially stratified estuary. J. Geophys. Res. 106 (C8), 17013–17037.
Uncles, R.J., Stephens, J.A., 2010. Turbidity and sediment transport in a muddy sub-estuary. Estuar. Coast. Shelf Sci. 87 (2), 213–224.

Van der Wegen, M., Jaffe, B.E., Roelvink, J.A., 2011. Process-based, morphodynamic hindcast of decadal deposition patterns in San Pablo Bay, California, 1856–1887. J. Geophys. Res.: Earth Surf. 116 (F2) (2003–2012).

Van Rompaey, A.J., Govers, G., Puttemans, C., 2002. Modelling land use changes and their impact on soil erosion and sediment supply to rivers. Earth Surf. Proc. Land. 27 (5), 481–494.

Wall, G.R., Nystrom, E.A., Litten, S., 2008. Suspended sediment transport in the freshwater reach of the Hudson River estuary in eastern New York. Estuar. Coasts 31 (3), 542–553.

Wang, L., Chen, S., 2001. Features of natural condition of Shenzhen Bay and problems needed to pay attention to during improvement. Pearl River 2001 (6), 4–7 (in Chinese).

Woodruff, J.D., Geyer, W.R., Sommerfield, C.K., Driscoll, N.W., 2001. Seasonal variation of sediment deposition in the Hudson River estuary. Mar. Geol. 179 (1), 105–119.

Wu, W., 2004. Depth-averaged two dimensional numerical modeling of unsteady flow and nonuniform sediment transport in open channels. J. Hydraul. Eng. 130 (10), 1013–1024.

Yue, S., Pilon, P., Cavadias, G., 2002. Power of the Mann Kendall and Spearman's rho tests for detecting monotonic trends in hydrological series. J. Hydrol. 255 (1–4), 254–271.

Zhang, Q., Liu, C., Xu, C., Xu, Y., Jiang, T., 2006. Observed trends of annual maximum water level and streamflow during past 130 years in the Yangtze River basin, China. J. Hydrol. 324 (1–4), 255–265.

Zhang, S., Duan, J.G., 2011. 1D finite volume model of unsteady flow over mobile bed. J. Hydrol. 405 (1), 57–68.

Zhang, W., Ruan, X., Zheng, J., Zhu, Y., Wu, H., 2010. Long-term change in tidal dynamics and its cause in the Pearl River Delta, China. Geomorphology 120 (3–4), 209–223.